Spectroscopy of strongly localized excitons and band-gap states in semiconducting single-walled carbon nanotubes

E. S. Comfort, D. A. Jones, A. Malapanis, Z. R. Robinson, M. T. Fishman, and J. U. Lee

Phys. Rev. B **83**, 081401 — Published 4 February 2011

DOI: 10.1103/PhysRevB.83.081401

Spectroscopy of Strongly Localized Excitons and Band Gap States in Semiconducting Single-Walled Carbon Nanotubes

E. S. Comfort[*], D. A. Jones[*], A. Malapanis[*], Z. R. Robinson[*], M. T. Fishman, and J.U. Lee[†]

College of Nanoscale Science and Engineering
University at Albany-SUNY, Albany, NY 12203, USA

Abstract:

It is often assumed that single-walled carbon nanotubes (SWNTs) grown via catalytic chemical vapor deposition (CVD) are free of defects, particularly when suspended over a trench. Here, we show that semiconducting nanotubes grown in this manner can contain a surprisingly large number of states within the band gap. High-resolution photocurrent spectroscopy is used to probe these states in individual nanotubes. We observe a series of band gap states in suspended nanotubes, resulting in long trapping and detrapping times. These states significantly alter the exciton spectra, resulting in a manifold of strongly localized exciton states with narrow line widths (<1 meV at room temperature) within a broader exciton envelope.

A fundamental understanding of the electronic and optical properties of any semiconductor needs to account for defects, which are often unavoidable and can mask the intrinsic properties of a semiconductor. Defects cause carrier scattering, serve as non-radiative recombination centers for electrons and holes, and alter the optical response of semiconductors. Single-walled carbon nanotubes are presumed to be ideal quasi-one-dimensional materials, exhibiting ballistic transport [1,2], excitonic effects [3], and electroluminescence [4,5]. While some evidence supports the presence of defects in non-suspended SWNTs [6,7], the detailed nature of these defects has not been presented. The prevailing view, moreover, is one in which suspended SWNTs are pristine, thus allowing the measurement of intrinsic properties. Evidence for this includes enhanced electroluminescence [8] and brighter photoluminescence [9] from suspended nanotubes when compared to non-suspended nanotubes. Here, we show that a series of band gap resonances is present in suspended semiconducting SWNTs. High-resolution photocurrent spectroscopy is used to probe these states in individual SWNTs in a p-n diode configuration. Band gap states lead to a manifold of strongly localized (bound) exciton states within a broader exciton envelope, with resonances that can be as narrow as 0.5 meV at room temperature. These results represent, to our knowledge, the first detailed spectroscopic study of band gap states in SWNTs.

To study the photoresponse of individual SWNTs, we have fabricated p-n diodes as shown in Fig. 1(a). The fabrication and characterization of p-n junctions in carbon nanotubes has been discussed elsewhere [10,11]. The current-voltage characteristics of our p-n diodes are similar to those reported previously, exhibiting good diode behavior with nearly ideal diode characteristics [10]. When a field effect transistor (FET) is biased in the on-state, the transport properties are unaffected by deep band gap states since the

Fermi energy is well above the filled states. Our structures can also be configured as a FET by using only the substrate as the gate. In this configuration, our devices operate just like any other nanotube FET and the band gap states cannot be probed. When biased as a diode, however, the undoped properties can readily be studied as we report in this letter.

In our previous studies, we have shown that these diodes can be used to measure the E_{11} and E_{22} transitions [12], the lowest exciton levels for the two lowest subbands. This is also used to confirm that we are measuring the properties of individual nanotubes. The key feature that allows the measurement of photocurrent from a single nanotube is its suspension over a trench. Photoluminescence at E_{11} energies has not been observed in non-suspended nanotubes [9], presumably due to substrate-induced defect states acting as non-radiative recombination centers. Similarly, in our studies, photoresponse is observed only in suspended nanotubes, which we have confirmed by fabricating and measuring non-suspended diodes that are otherwise identical to our suspended diodes – i.e. no photoresponse is observed in non-suspended nanotubes.

We would also like to point out other unique features of our measurements. First, the optical power density we use is at least 1000 times lower than power densities used in nearly all other single nanotube studies, reducing the likelihood of photo-induced desorption of adsorbates. Second, some have reported broadening of the exciton line-width with increased excitation power. The low power density that we use, therefore, could partly explain the significantly reduced line-widths observed in our measurements. The most significant attribute of our measurement is the absence of homogenous broadening that is likely to be present in measurements of many nanotubes.

Two different optical sources are used to measure the photocurrent spectra. For measuring spectra over a broad energy range (0.5-2 eV), a Quartz Tungsten Halogen lamp is used with a monochromator. With this setup, the E_{11} and E_{22} excitonic transitions of a single SWNT can be determined, allowing for unambiguous diameter assignment. To maximize the power output, the bandwidth is set high by widening the inlet and outlet slits of the monochromator. This results in a spectral resolution of 5 nm, which corresponds to 3-6 meV over the scan range. In the second setup, we examine high-resolution photocurrent spectra using a mode-hop-free CW tunable laser that can scan continuously from 1260-1630 nm (0.761-0.984 eV) with a resolution of <10 pm (Santec, model TSL-210VF). The high resolution and higher optical power of the laser (300 mW/cm^2), combined with the low noise of our photocurrent measurement setup, allow for detailed examination of band gap states not possible with the broadband source. Our results are typical of many nanotubes examined. All measurements were performed in air at 300 K. Photocurrent spectra taken with the laser is measured at constant power since we expect at most 20% change when converting from constant power to constant flux over the scan range.

Before continuing, it is important to properly reference the energy levels we are able to probe with the laser. Since an exciton is formed from a bound electron and hole, the lowest exciton level is separated from the continuum (the band gap) by the binding energy. A key question in our study is how the energy of the first subband gap relates to the energy range of our laser. In a recent study, high-resolution scanning tunneling spectroscopy of a nominal nanotube, 1.4 nm in diameter, yielded a band gap of 1.05 eV [13], suggesting a band gap scaling behavior of $1.5/d$ eV/nm, where d is the diameter of the nanotube. This is in good agreement with our previous optical study, in which we

have measured a band gap scaling of 1.55/*d* eV/nm [12]. For the nanotube diameters that we grow, which range from 1.3-1.8 nm, we conclude that the energy range of our laser falls within the band gap of the lowest subband. Diameter assignment is further corroborated by measuring E_{11} and E_{22} levels, which readily allows diameter assignment using a Kataura plot [14]. Since measurements and detailed many-body calculations predict an exciton binding energy that can be a significant fraction of 1 eV [3, 15, 16], the exciton levels also provide a good measure of the continuum. In the absence of band gap states, we expect only a handful of optically excited states between the E_{11} level and the continuum. Here, we show that these states alter the expected photocurrent spectral response within this range, which is the central result of our paper.

Fig. 1(b) shows the laser spectra taken from two sequential scans of a single device. The sharp peaks are narrow resonances, nearly all of which are reproducible. For this nanotube, the E_{11} and E_{22} levels measured with the spectrometer are 0.671 eV and 1.298 eV, respectively, allowing us to assign the nanotube diameter of approximately 1.5 nm. In this diameter range, our laser is able to probe well below the continuum level of ~1 eV. Fig. 1(c) is a close-up region of the scan in Fig 1(b) showing that the narrow resonances are reproducible in every detail. We again note that these resonances are much weaker than the E_{11} and E_{22} levels and are not visible in the scan with the monochromator (See figure 4 and reference 12).

Photocurrent in a similar device structure showed little current from the doped regions [17], confirming that the photocurrent is generated from the region between the split gates. In Fig. 1(c), approximately 30 different peaks are observed. The possibility that other excitonic states are responsible for these peaks is ruled out by the large number of resonances that are observed. With unequal K and K' points in the Brillouin zone,

there can be at most 16 exciton levels, not all of which are optically active [18]. Therefore, the observed resonances in Fig. 1 cannot be accounted for by these additional exciton states, even through the influence of symmetry-breaking processes that allow them to be optically active [19]. Indeed, these resonances are characteristic of localized band gap states, which we reveal here for the first time.

The spacing between resonances is correlated and varies from nanotube to nanotube. In Fig. 2, we show the autocorrelation of one particular spectrum with a repeat spacing of ~5 meV. This spectrum was chosen because it showed a large window with similar peak values. The autocorrelation of our signal is given as $y(m) = \sum_{n=1}^{N} f(n) f(n-m)$ where $f(n)$ is the value of the photocurrent at energy n. For meaningful correlation, sampling as defined by lag m (ΔE) is over about 1/4 of the total spectrum N. The autocorrelation is normalized for clarity. The correlation is likely a signature of defects, though presently we can only speculate about the nature of these states.

To further investigate the nature of these band gap states, we examined the detrapping current when the laser illumination is switched off (Fig. 3). The photocurrent is observed to decay with multiple time constants that range between 5-10 s. Using a calibrated InGaAs photodiode, we verified that the optical power from the laser source can be turned off within 1 s, confirming that the nature of the long decay is intrinsic to the nanotubes, and that the laser spectrum is featureless, without the presence of narrow peaks. The large decay constant is consistent with deep localized states within the band gap. To examine the origin of the decay times, we use a phenomenological approach based on the Shockley-Read-Hall (SRH) theory [20]. Extending this analysis to a one-dimensional (1D) semiconductor, the emission time constant is given as

$\tau_{emission}^{-1} = v_{th} n_i \exp\left(\frac{E_t - E_i}{kT}\right)$, where v_{th} is the thermal velocity, n_i is the band gap-dependent intrinsic carrier concentration, k is Boltzmann's constant, and T is the temperature; E_t and E_i are the trap energy and intrinsic energy levels, respectively. We use the universal density of states of nanotubes [21] to calculate the intrinsic carrier density. Fitting the data to the 1D SRH theory, we calculate trap energy levels of 0.35-0.37 eV below the intrinsic level for a band gap of 1 eV. While this confirms that deep band gap states are involved, we note that the above analysis is taken in the limit of lower disorder and may overestimate the trap levels for highly disordered semiconductors. The important conclusion is that narrow resonances are seen with correlated spacing throughout the energy range explored in measurements, up to almost 1eV.

To illustrate the carrier dynamics in the presence of band gap states, we show the filling and emptying of photoexcited carriers in the inset of Fig. 3 [22]. At equilibrium, defect states below the Fermi level are occupied, resulting in trapped states, while states above the Fermi level are empty. Under illumination, the occupied band gap states depopulate by absorbing photons. These carriers are excited into the conduction band, generating a photocurrent. At the same time, electrons in the valence band are excited into the unoccupied band gap states above the Fermi level, leaving behind free holes that add to the photocurrent. When illumination is switched off, band gap levels that were occupied above the Fermi level detrap. Any band gap levels below the Fermi level that were emptied during the photoexcitation will be filled by valence band states. These two processes give rise to exponentially decaying currents with time constants given by $\tau_{emission}$.

The presence of band gap states has a striking effect on the exciton spectra. Fig. 4(a) shows spectra taken with both the broadband and laser sources on a nanotube with an E_{11} level within the scan range of the laser. Other than a satellite peak 27 meV below the primary peak (outside the scanning range of the laser), the broadband source is not able to resolve the manifold of resonances that the laser is able to identify. In Fig. 4(b), we show a close-up of the E_{11} peak for two sequential laser scans to show the stability of these resonances. The manifold of peaks within a broader exciton envelope is explained from the direct formation of localized excitons from band gap states. The extremely narrow resonances are consistent with localized excitons since the kinetic energy contribution to line-width broadening vanishes.

Within an effective mass approximation, localization in position implies delocalization in momentum states of an exciton, resulting in a flat dispersion relation. This results in narrower spectra compared to a delocalized exciton. Narrowing of line-widths for bound excitons are also observed in other low dimensional semiconductors [23, 24]. We attribute the satellite peak to additional localized exciton states which have been observed also by others [5, 25].

Although we cannot determine the physical origin of the band gap states in our nanotubes, single vacancies, topological deviations, adsorbates and a host of other defects have been shown to create these states [26]. Within this picture, the manifold of exciton states can be formed either from charged defect states that create localized excitons through attractive dipole-monopole interactions or from a localized exciton where one of the constituent carriers is tightly bound to a defect while the other carrier forms hydrogen-like levels. It is likely that a combination of these effects contribute to the abundance of the narrow absorption lines. In the ideal limit of a single delta impurity

potential, localization of an exciton with energy below the bright exciton has been calculated recently with energy splitting similar to those shown in the manifold of exciton peaks of Fig. 4 [27]. Localized excitons are depicted in the inset of Fig. 4(b).

In summary, we show the presence of narrow band gap resonances using high-resolution photocurrent spectroscopy in seemingly pristine SWNTs. We attribute the band gap states to the presence of defects along the suspended region. The defect states greatly alter the first exciton peak, splitting it into a manifold of peaks created by localized excitons. Further studies of defect states are in progress to determine the exact nature of the defects and the mechanism of bound excitons.

This work was supported by NSF grant number EPDT-0823715 and DTRA grant number HDTRA1-10-1-0016. We would like to thank Y. Tomio, S. Rotkin, and S. Oktyabrsky for useful discussions.

Figure Captions

FIG. 1 (Color Online). (a) Schematic of our structure to investigate band gap spectroscopy of individual carbon nanotubes. The two gates $V_{g1,2,}$ are separated by 0.5-1.5 μm and are oppositely biased (+/-5V) to create separate regions of p-and n-type doping along a nanotube. The top gate dielectric is SiO_2 with a thickness of 25nm. This geometry and applied bias result in a doping density of 0.6 carriers/nm which result in degenerately doped p- and n-doped regions. (b) Two sequential laser spectra of a carbon nanotube p-n diode biased at zero volts showing resonances due to band gap states. For this nanotube, E_{11}=0.671 eV and E_{22}=1.298 eV, which correspond to diameters of either 1.51 or 1.54 nm, as discussed in the text. (c) A 50 meV window of the scan in (b), showing that nearly all of the resonances are reproducible. Measurements are taken in air at 300 K with the laser scanned in 1nm increments at a constant power of 300mW/cm^2.

Fig. 2 (Color Online). Autocorrelation of a nanotube showing correlated peak positions spaced by ~5 meV. A photocurrent spectrum is shown in the inset (scanned with 0.2 nm increments at a constant power of 300mW/cm^2).

FIG. 3 (Color Online). Detrapping current after the laser light is turned off at t=0, showing multiple time scales corresponding to emission from deep band gap states. Inset: Vertical transition (↑) denoting optical excitation of carriers into and out of trap states. After the laser is switched off, thermal excitation (↺) of carriers fill or empty band gap states that were out of equilibrium during photoexcitation. The thermal excitation gives rise to the energy-dependent detrapping current. Laser was set at 0.761eV, 3W/cm^2 prior to turning it off.

Fig. 4 (Color Online) (a) Photocurrent spectra taken with both a broadband source and a laser near the E_{11} transition. The E_{11} resonance taken with a laser shows a manifold of peaks that are due to localized excitons associated with defect states, as shown in the inset of (b). Just as in Fig. 1, the band gap states measured with the laser are reproducible in every detail. (b) Close-up scan of the E_{11} resonance taken from two sequential laser scans. While both trapped carriers and localized excitons give rise to discrete peaks in the photocurrent, the exciton spectrum has a qualitatively different behavior than the band gap states. Measurements are taken in air at 300 K with spectra taken in 1nm steps at a power of 250mW/cm^2. The nanotube diameter is 1.4nm.

Figure 1

(a)

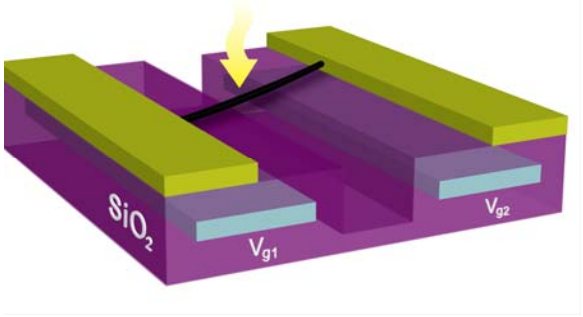
SiO2
Vg1
Vg2

(b)

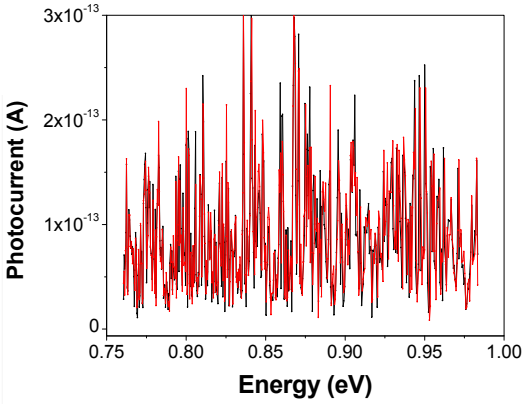
3x10-13
2x10-13
1x10-13
0
Photocurrent (A)
0.75
0.80
0.85
0.90
0.95
1.00
Energy (eV)

(c)

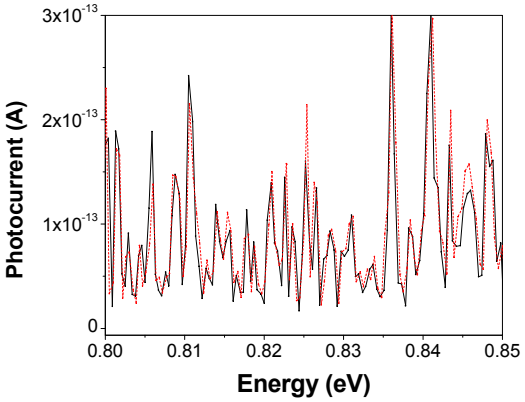
3x10-13
2x10-13
1x10-13
0
Photocurrent (A)
0.80
0.81
0.82
0.83
0.84
0.85
Energy (eV)

Figure 2

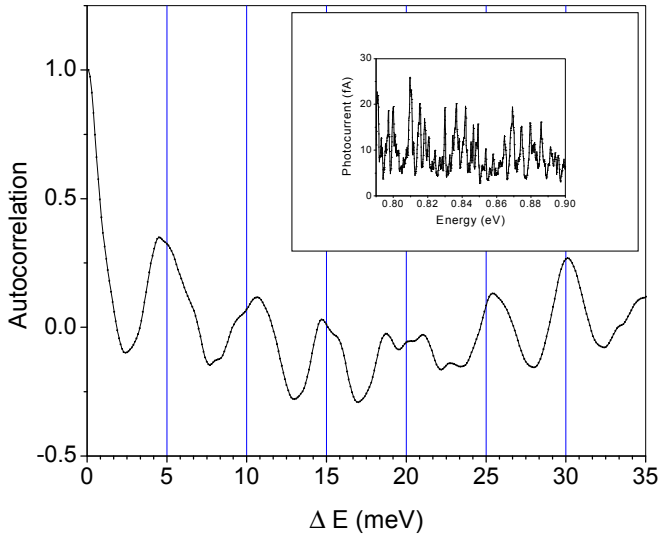
Autocorrelation
1.0
0.5
0.0
-0.5
0
5
10
15
20
25
30
35
Δ E (meV)
Photocurrent (fA)
30
20
10
0
0.80
0.82
0.84
0.86
0.88
0.90
Energy (eV)

Figure 3

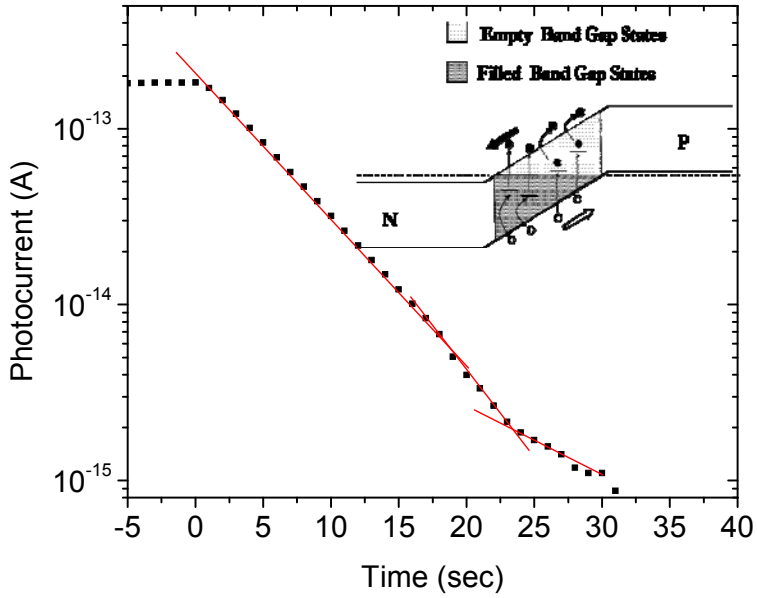
Empty Band Gap States
Filled Band Gap States
P
N
Photocurrent (A)
10^-13
10^-14
10^-15
-5
0
5
10
15
20
25
30
35
40
Time (sec)

Figure 4

(a)

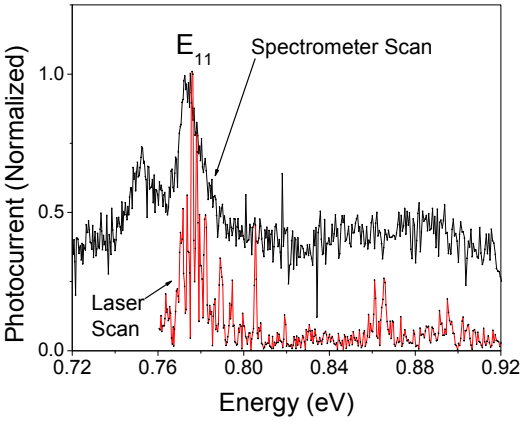
E11
Spectrometer Scan
Laser
Scan
Photocurrent (Normalized)
1.0
0.5
0.0
0.72
0.76
0.80
0.84
0.88
0.92
Energy (eV)

(b)

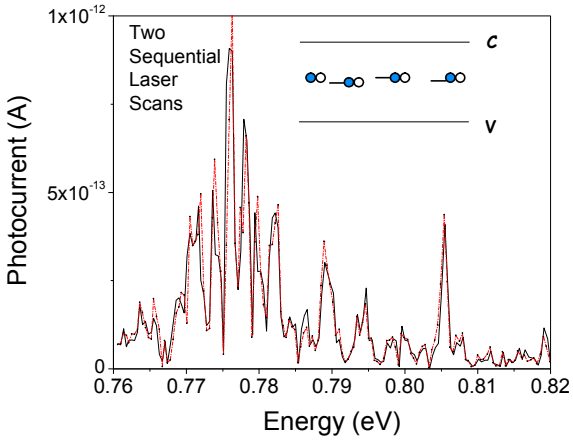
1x10-12
Two
Sequential
Laser
Scans
c
v
Photocurrent (A)
5x10-13
0
0.76
0.77
0.78
0.79
0.80
0.81
0.82
Energy (eV)

* These authors contributed equally to this work
† Corresponding author: jlee1@uamail.albany.edu

[1] A. Javey, J. Guo, Q. Wang, M. Lundstrom, and H. Dai, Nature (London) **424**, 654 (2003).

[2] A. Javey, J. Guo, D. Farmer, Q. Wang, E. Yenilmez, R. Gordon, M. Lundstrom, and H. Dai, Nano Letters **4,** 1319 (2004).

[3] F. Wang, G. Dukovic, L. Brus, and T. Heinz, Science, **308**, 838 (2005).

[4] J. A. Misewich, R. Martel, Ph. Avouris, J.C. Tsang, S. Heinze, and J. Tersoff, Science **300**, 783 (2003).

[5] T. Mueller, M. Kinoshita, M. Steiner, V. Perebeinos, A.A. Bol, D.B. Farmer, and Ph. Avouris, Nature Nano. **5**, 27 (2010).

[6] P. McEuen, M. Bockrath, D.H. Cobden, Y.G. Yoon, and S.G. Louie, Phys. Rev Lett. **83**, 5098 (1999).

[7] Y. Fan, B.R. Goldsmith, and P.G. Collins, Nature Mat. **4**, 906 (2005).

[8] J. Chen, V. Perebeinos, M. Freitag, J. Tsang, Q. Fu, J. Liu, and Ph. Avouris, Science **310**, 1171 (2005).

[9] J. Lefebvre, Y. Homma, and P. Finnie, Phys. Rev. Lett. **90**, 217401 (2003).

[10] J.U. Lee, P. Gipp, and C.M. Heller, App. Phys. Lett. **85**, 145 (2004).

[11] K. Bosnick, N. Gabor, and P. McEuen, App. Phys. Lett. **89**, 163121 (2006).

[12] J.U. Lee, P. J. Codella, and M. Pietrzykowski, Appl. Phys. Lett. **90**, 053103 (2007).

[13] H. Lin, J. Lagoute, V. Repain, C. Chacoon, Y. Girard, J.S. Lauret, F. Ducastelle, A. Loiseau and S. Rousset, Nature Mat., **9**, 235 (2010).

[14] P.T. Araujo, P.B.C. Pesce, M.S. Dresselhaus, K. Sato, R. Saito and A. Jorio, Physica E **42**, 1251 (2010).

[15] C.D. Spataru, S. Ismail-Beigi, L.X. Benedict, and S.G. Louie, Phy. Rev. Lett. **92**, 077402 (2004).

[16] V. Perebeinos, J. Tersoff, and Ph. Avouris, Phys. Rev. Lett. **92,** 257402 (2004).

[17] N. Gabor, Z. Zhong, K. Bosnick, J. Park, P. McEuen, Science **325**, 1367 (2009).

[18] T. Ando, J. Phys. Soc. Japan **75**, 024707 (2006).

[19] H. Harutyunyan, T. Gokus, A.A. Green, M.C. Hersam, M. Allegrin, and A. Hartschuh, Nano Lett. **9**, 2010 (2009).

[20] W. Shockley and W.T. Read, Phys. Rev. **87**, 835 (1952).

[21] J.W. Mintmire and C. T. White, Phys. Rev. Lett. **81**, 2506 (1998).

[22] In the band diagram, we ignore the band gap renormalization in the doped regions as has been calculated recently in C.D. Spataru and F. Leonard, Phys. Rev. Lett. **104**, 177402 (2010).

[23] D. Gammon, E.S. Snow, B.V. Shanabrook, D.S. Katzer and D. Park, Phys. Rev. Lett. **76**, 3005 (1996).

[24] F. Intonti, V. Emiliani, C. Lienau, T. Elsaesser, V. Savona, E. Runge, R. Zimmermann, R. Notzel and K.H. Ploog, Phys. Rev Lett. **87**, 076801 (2001).

[25] O. Kiowski, K. Arnold, S. Lebedkin, F. Hennrich and M.M. Kappes, Phys. Rev. Lett. **99**, 237402 (2007).

[26] See for example: J.C. Charlier, X. Blasé, and S. Roche, Rev. Mod. Phys. **79**, 677 (2007).

[27] Y. Tomio and H. Suzuura, Physica E, **42**, 783 (2010).